

## Modelling and mapping soil organic carbon stocks under future climate change in south-eastern Australia



Bin Wang <sup>a,\*</sup>, Jonathan M. Gray <sup>b</sup>, Cathy M. Waters <sup>c</sup>, Muhuddin Rajin Anwar <sup>a,d</sup>, Susan E. Orgill <sup>a</sup>, Annette L. Cowie <sup>e</sup>, Puyu Feng <sup>f</sup>, De Li Liu <sup>a,g</sup>

<sup>a</sup> NSW Department of Primary Industries, Wagga Wagga Agricultural Institute, Pine Gully Road, Wagga Wagga, NSW 2650, Australia

<sup>b</sup> NSW Department of Planning, Industry and Environment, PO Box 644, Parramatta, NSW 2124, Australia

<sup>c</sup> NSW Department of Primary Industries, 34 Hampden Street, Dubbo, NSW 2830, Australia

<sup>d</sup> Graham Centre for Agricultural Innovation (an alliance between NSW Department of Primary Industries and Charles Sturt University), Pine Gully Road, Wagga Wagga, NSW 2650, Australia

<sup>e</sup> NSW Department of Primary Industries, Trevenna Rd, Armidale, NSW 2351, Australia

<sup>f</sup> College of Land Science and Technology, China Agricultural University, Beijing 100193, China

<sup>g</sup> Climate Change Research Centre, University of New South Wales, High Street, Sydney, NSW 2052, Australia

### ARTICLE INFO

Handling Editor: Budiman Minasny

**Keywords:**

Soil organic carbon  
Global climate models  
Climate change  
Multiple linear regression  
Random forest  
South-eastern Australia

### ABSTRACT

Soil organic carbon (SOC) plays a key role in the sequestration of carbon that could otherwise be warming the atmosphere. Climate change including increased temperature and changed rainfall will greatly impact the global SOC cycle. There are still significant gaps in our knowledge of the size of the global SOC pool and how future climate will affect SOC stocks and flows in many parts of the world, including Australia. In this study, we used SOC data in a Digital Soil Mapping framework to predict current and future SOC stocks across the state of New South Wales (NSW) in south-eastern Australia. In the first phase of the study we estimated the current SOC stock using multiple linear regression (MLR) and random forest (RF) modelling, and in the second phase we projected the change of SOC stocks in the near future (2050s) and far future (2090s) under two Shared Socio-economic Pathways (SSPs) scenarios based on 25 global climate models (GCMs) from the Coupled Model Inter-comparison Project Phase 6 (CMIP6). Our spatial modelling showed that estimated current SOC stocks in NSW decreased from east to west. Multi-GCM ensemble means suggested SOC stocks would decrease by 7.6–12.9% under SSP2-4.5 and 9.1–20.9% under SSP5-8.5 across NSW under future climate. The extent of change in SOC stocks varied spatially with the largest mean decrease of SOC stocks occurring in the North Coast and South East (alpine) regions of NSW. Our findings can support decision-making in land management and climate change mitigation strategies in NSW at the regional level. Furthermore, the modelling methods can be applied to other areas where edaphic and landscape properties, land use, and climate data are available.

### 1. Introduction

Soil organic carbon (SOC) is recognised as the most important indicator of soil fertility and productivity because it reflects the level of soil organic matter, which affects plant growth through its influence on nutrient cycling, water availability, and soil structural stability (Schmidt et al., 2011). Soil plays a vital role in the global carbon (C) cycle, storing approximately twice the amount of C than the atmosphere and about three times that of terrestrial vegetation (Smith, 2012). Small percentage changes in the SOC pool can significantly affect the global C cycle, influencing the content of carbon dioxide in the atmosphere. Therefore

SOC has profound implications for the mitigation of global climate change (Stockmann et al., 2013).

Reliable assessment of SOC stocks at different spatiotemporal scales is critical to understanding the impacts of future climate change on SOC dynamics. Digital Soil Mapping (DSM) techniques comprise various multivariate statistical methods that utilise the relationship between measured soil properties and numerous predictor variables measured at the same sites to create a spatial soil information system (McBratney et al., 2003). The multiple linear regression (MLR) method has been widely used as a DSM technique to estimate stocks of SOC. The advantage of MLR is its simplicity and straight-forward intuitive interpretation

\* Corresponding author.

E-mail address: [bin.a.wang@dpi.nsw.gov.au](mailto:bin.a.wang@dpi.nsw.gov.au) (B. Wang).

(Rial et al., 2017). Numerous studies have applied non-linear models through machine learning methods for DSM of SOC stocks (Padarian et al., 2020; Wadoux et al., 2020). For example, Grimm et al. (2008) used random forest (RF) and Wang et al. (2018a) used boosted regression trees and support vector machines to relate SOC stocks to environmental auxiliary variables. These machine learning models have proven more accurate and powerful in estimating and mapping current SOC stocks than MLR (Forkuor et al., 2017; Gray et al., 2019).

Estimating the total SOC stocks in different regions of Australia has largely been undertaken by different DSM techniques (Bennett et al., 2020; Gray et al., 2015; Somaratna et al., 2016). For example, Gray et al. (2019) used both MLR and RF models with multiple datasets to estimate SOC stocks to 30 cm in New South Wales (NSW), achieving Lin's concordance correlation coefficients (LCCC) up to 0.79. Wang et al. (2018a) developed different DSM techniques to predict SOC stocks in the semi-arid rangelands of eastern Australia using high spatial resolution satellite data (seasonal fractional cover data) together with other environmental covariates. Their model had a moderate performance in estimating SOC stocks at 0–30 cm with the correlation coefficient being 0.66. Additionally, they reported that rainfall is the most important predictor of total SOC stock. Viscarra Rossel et al. (2014) used decision tree modelling to map SOC stocks to 30 cm across the Australian continent, achieving a mean LCCC of 0.81. These studies provide valuable information for estimating SOC stocks in Australia using various environmental covariates. However, there is a need for validating different DSM models against observed data before predicting future changes in SOC stocks under climate change.

Climate change is expected to have significant effects on the stocks and flows of SOC because changes in temperature and seasonal rainfall patterns can influence the amount and rate of organic matter (OM) supply and decomposition (Soleimani et al., 2017). Understanding the relationship between climate and SOC accumulation is critical to quantifying the potential for climate change mitigation through SOC management, and can inform land use and management decisions which can ultimately lead to more resilient agricultural production systems (Lal, 2004). Towards this, numerous researchers have investigated the response of SOC stocks to changes in climatic conditions (e.g. Adhikari et al. (2019) and Rial et al. (2017)). There is an overall increase in global SOC stocks in the 21st century projected by process-based vegetation C models under climate change, however, the extent of SOC change varies with climate models and emission scenarios for different regions (Gottschalk et al., 2012; Lucht et al., 2006). These simulated differences in change in SOC stocks among studies relate to the complex interrelationships between the factors that determine the C balance of soils in biophysical models and uncertainties in future climate projections. Based on various DSM approaches, previous studies have also used different global climate models (GCMs) to study the impacts of climate change on SOC stocks for different countries (Lozano-García et al., 2017; Yigini and Panagos, 2016). For instance, Yigini and Panagos (2016) employed a geostatistical model to predict future SOC stocks in Europe based on four GCMs under four representative concentration pathways (RCPs) and found an overall increase in SOC stocks by 2050 in Europe for all climate scenarios. Olaya-Abril et al. (2017) reported that SOC concentration in southern Spain may decline by 35.4 % under a high emission scenario. Gray and Bishop (2019) applied a DSM approach to examine and map the potential change in SOC stocks with 12 climate models in eastern Australia. They reported that future SOC stocks would decrease over the study area, however the magnitude of decline varied with different climate projections. The major limitation of these previous studies is that they selected a limited number of GCMs from Coupled Model Inter-comparison Project phase 5 (CMIP5) to represent future climate projections in the DSM. There are large variations between future climate projections, especially in seasonal rainfall, from different GCMs (CSIRO and BoM, 2015). The use of too few climate models can result in overconfidence if they have strong dependence (Knutti, 2010). Numerous studies concluded that using a multi-GCM ensemble under

different emission scenarios provides a more robust assessment of climate change impact (Knutti, 2010; Lobell et al., 2015).

The future climate projections from multiple GCMs indicate that annual mean temperature will continue to increase, with drier winters and wetter summers in south-eastern Australia (CSIRO and BoM, 2015; Feng et al., 2019). Additionally, Ukkola et al. (2020) found that CMIP6 projections indicate a greater probability of meteorological drought compared with CMIP5 projections. CMIP6 should provide less biased simulations for use in regional dynamical and statistical downscaling efforts compared with CMIP5 (Cannon, 2020). The effects of climate change on SOC can be critical in Australia since climate is the most important driver of SOC stocks (Bennett et al., 2020; Robertson et al., 2016). Knowledge of how future climate change might affect SOC stocks is crucial to developing management strategies that minimise SOC decline (Adhikari et al., 2019). Nonetheless, as far as we are aware, no study has used DSM to assess potential change in SOC stocks using climate models based on CMIP6 under different emission scenarios in Australia or elsewhere.

In this study, we used multiple sources of legacy SOC data with a range of environmental covariates to quantify the spatiotemporal dynamics of SOC stock using DSM techniques in the state of NSW in south-eastern Australia. We aimed to provide robust projected results, therefore we used 25 available GCMs from the CMIP6 projections under different emission scenarios to cover a large range of change in the climate variables of temperature and rainfall. Our objectives were to (1) develop different DSM methods to estimate and map current SOC stocks in south-eastern Australia, (2) predict the change in SOC stocks under future climate and (3) investigate the relationship between SOC stock change and climate change. The assessment of the impacts of future climate change on total SOC stocks across NSW and understanding its environmental controls are important to predict the region's response to global climate change and develop climate mitigation strategies to meet the net zero emission target for NSW.

## 2. Materials and methods

### 2.1. Study area

The study area was located in the state of NSW in the southeast Australia, which has an area of approximately 800,000 km<sup>2</sup>. The state has a wide range of environments with 18 bioregions that vary considerably in vegetation communities, landform, and soil type (Bioregions NSW, 2021). It has a temperate monsoon climate; its mean annual rainfall is <300 mm in the west and more than 1500 mm in the northeast coastal region, and mean annual temperature ranges from 3 to 21 °C (<http://www.bom.gov.au/climate/>). The majority of the land in NSW is occupied by grazing (63 %), dryland cropping (15 %), and nature conservation (13 %) (ABARES, 2021). The main soil types according to the Australian Soil Classification System (ASCS) are Chromosols, Vertosols, and Tenosols. The soils in NSW are characterized by low fertility and poor physical conditions in the west. There are higher SOC concentration and fertility in the east, related to differences in parent material and rainfall. Within NSW, there are 11 natural resource management regions, known as Local Land Service (LLS) regions (Table 1).

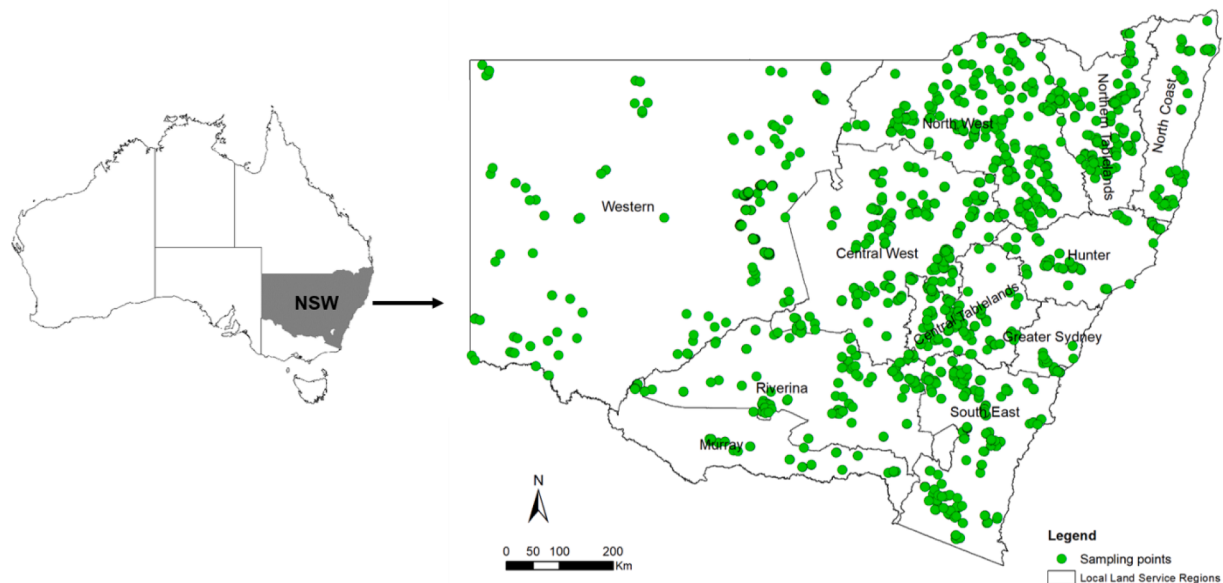
### 2.2. Observed soil data

The SOC dataset was prepared using 2153 points (Fig. 1) sourced from the following projects: (1) NSW Monitoring, Evaluation and Reporting (MER) program of the NSW Government during 2008–09 (OEH, 2014); (2) National Soil Carbon Research Program (SCaRP) 2009–2012 (Sanderman et al., 2011) and (3) Filling the Research Gap - National Soil Carbon Research Program (2014–2017) (Waters et al., 2015; Waters et al., 2016).

Each data point represented a soil core divided into depths of 0–10 cm, 10–20 cm, and 20–30 cm (Projects 1 and 2) or 0–5 cm, 5–10 cm,

**Table 1**The 11 Local Land Service (LLS) regions in NSW (<https://www.lls.nsw.gov.au/>).

LLS regions	Agricultural industries	Area (km <sup>2</sup> )	Mean temperature (°C)	Rainfall (mm)
Central Tablelands	Temperate climate with equiseasonal rainfall supporting productive grazing (red meat and wool) and cropping with some irrigated cropping and horticulture. Soils are largely red and yellow duplex soils and fertile red gradational soils with small areas of black cracking clays.	31,347	14.4	727
Hunter	Temperate climate with productive grazing (red meat, wool and dairy) and poultry, with some dryland cropping on alluvial soils. Soils are sandy alluvial flats, to deep friable loams and red duplex soils.	33,006	17.0	887
North Coast	Temperate and subtropical climate supporting productive grazing (red meat, wool and dairy), poultry, soybeans, sugar, tea tree and coffee. Soils are red, yellow and brown duplex soils, fertile red and brown gradational soils, deep siliceous sands and small areas of black cracking clays.	32,060	18.3	1245
Northern Tablelands	Highland region with temperate climate supporting productive grazing (red meat and wool) and cropping (cereals, legumes and oil seeds). Soils are yellow duplex and sandy soils and fertile red gradational soils.	39,509	15.0	825
South East	Temperate and warm temperate climate in a diverse region including: alpine, coast and tablelands environments that support productive grazing (red meat, wool and dairy), cropping and horticulture. Soils are diverse and include: structureless uniform soils, red, yellow and brown duplex soils and fertile brown gradational soils.	55,627	13.3	776
Western	Semi-arid to arid with low and highly variable rainfall where drought is a major part of the climatic cycle. Main agricultural land use is grazing (red meat and wool), with some cropping in the southern Mallee and irrigated agriculture (cotton, horticulture and viticulture). Soils are gradational calcareous, fertile red and brown gradational soils, structureless sands and cracking clays.	314,493	19.7	285
Riverina	Semi-arid to temperate climate supporting grazing (red meat and wool) and cropping in the west, fruit growing and dairying on the south-eastern slopes and irrigated horticulture, grain, rice and forages. Soils are red, grey and yellow duplex soils, fertile brown gradational soils and small areas of cracking clays.	67,083	16.5	490
Murray	Temperate climate supporting grazing (red meat, wool and dairy) and cropping with some irrigated horticulture and crops. Soils are red, grey and yellow duplex soils and fertile brown gradational soils.	41,899	15.9	501
Greater Sydney	Warm temperate climate supporting intensive industries such as market gardens, poultry and turf. This is the most intensely urbanised locality in NSW. Soils are typically sandy grey and brown duplex soils and fertile gradational and alluvial soils.	12,497	16.6	951
Central West	Warm and temperate climate supporting grazing (red meat and wool) and cropping (cereals, legumes and oil seeds) often in mixed farming enterprises with some irrigated horticulture, cotton and dairy. Soils are red, grey and yellow duplex soils and fertile brown gradational soils.	91,619	18.1	512
North West	Warm and temperate climate supporting grazing (red meat and wool) and cropping (cereals, legumes and oil seeds) with some irrigated cropping (cotton). Soils are red, brown and yellow duplex soils, fertile brown gradational soils and large areas of cracking clays.	82,443	18.9	577

**Fig 1.** Location of the 2153 soil samples used for model development in New South Wales (NSW) with 11 Local Land Service Regions.

10–20 cm, and 20–30 cm (Project 3). Samples were oven dried to 40 °C, sieved to <2 mm to remove and account for gravel %, and SOC content (g C (100 g)<sup>-1</sup> sieved soil) was determined on approximately 2 g of finely ground soil analysed by dry combustion on a LECO combustion furnace (LECO 1995) (Rayment and Lyons, 2011; Method 6B2b). Bulk density (BD, g cm<sup>-3</sup>) was determined on the same cores using subsamples dried at 105 °C as described by Dane and Topp (2002).

For each soil core, SOC stock for each soil layer was calculated using

SOC concentration, gravel % and BD (Eq. (1)). To obtain the SOC stock to 30 cm soil depth, we summed SOC stocks for all layers 0–30 cm.

$$SOC_{stock}(t \text{ ha}^{-1}) = C \times BD \times D \times \left(1 - \frac{gravel[\%]}{100}\right) \quad (1)$$

where  $C$  is the concentration of soil carbon (g C (100 g)<sup>-1</sup> sieved soil);  $BD$  is bulk density of the whole soil (g cm<sup>-3</sup>);  $D$  is the thickness or depth of the corresponding soil layer (cm);  $gravel [\%]$  is the percentage of gravel

in the soil sample.

### 2.3. Environmental variables

Our study used environmental variables related to the key soil forming factors of climate, parent material, biota, topography, and age based on the ‘scorpan’ factors (McBratney et al., 2003). It should be noted that variables with strong correlation with climate were not included, such as fractional ground cover (vegetation indices) (Guerschman et al., 2015) and clay mineral proportions (Viscarra Rosser, 2011). This is because these predictors would not have remained constant into the future with the projected climate change, as required for the modelling, thus potentially distorting modelling results (Gray and Bishop, 2019).

All predictors used are listed in Table 2 and outlined in more detail below. First, the original spatial datasets for auxiliary variables, with the exception of temperature and rainfall, were resampled into raster format with the same 100 m resolution based on nearest neighbour resampling method. Then, the pixel values of each spatial layer were extracted for all 2153 sampling points, and finally, a database was built to develop prediction models.

#### 2.3.1. Topography

Slope (in percent) and aspect were derived from the Smoothed Digital Elevation Model (DEM-S) using the finite difference method (Gallant and Wilson, 2000). They were downloaded from CSIRO Data Access Portal (<https://data.csiro.au/collections>). We regressed the slope and aspect data to 100 m. Then the slope data together with an aspect (orientation) layer were used to derive a new 1–10 aspect index, as described in Gray et al. (2015). Sites that receive high solar radiation, such as on gentle slopes and those facing north and north-west, have low aspect indices, whereas sites that receive low solar radiation, such as those with steep south and south-easterly facing slopes, have high aspect indices.

Topographic wetness index (TWI) represents topographic influence on hydrological processes, based on slope and catchment area, as derived from the DEM-H (a hydrologically enforced model). The method and equations for deriving TWI were reported by Gallant and Austin (2002).

**Table 2**  
The 11 predictor variables used in predicting SOC stocks.

Types	Variables	Definition
<i>Topography</i>	Slope	Slope gradient (%) as derived from a digital elevation model (DEM)
	Aspect index	Approximation of the amount of solar radiation received by site
	Topographic Wetness Index (TWI)	Relative wetness due to terrain-factors within catchments, a measure of position on the slope with larger values indicating a lower slope position
<i>Biota</i>	Land disturbance index (LDI)	Intensity of disturbance associated with land use
<i>Age</i>	Weathering Index (WI)	Degree of weathering of parent materials, regolith and soil, based on gamma radiometric data
<i>Climate</i>	Rainfall (Rain)	Mean annual rainfall (mm)
	Minimum temperature (Tmin)	Mean annual minimum temperature (°C)
<i>Parent material</i>	Silica index	Class of silica content (%), indicating lithological character of the parent material. Surrogate for soil texture through the proportion of sand (silica) from weathering parent material
	Radiometric potassium (Rad_k)	Concentration of the radioelement potassium
	Radiometric uranium (Rad_u)	Concentration of the radioelement uranium
	Radiometric thorium (Rad_th)	Concentration of the radioelement thorium

(2015). We downloaded TWI through the CSIRO Data Access Portal (<https://data.csiro.au/collections>). The TWI dataset has an original resolution of 30 m and this was regressed to 100 m.

#### 2.3.2. Climate

Historical climate data were obtained from the SILO (Scientific Information for Land Owners) website (Jeffrey et al., 2001). There were 2096 climate stations available in NSW. For model development, we calculated annual mean minimum temperature (Tmin) and rainfall over the 30 years prior to date of sampling for all 2153 soil sites, using the climate data from the nearest climate stations. A 30-year period is the accepted convention to characterise climate (WMO, 2017). For the spatial map preparation, we interpolated historical annual mean of Tmin and rainfall in the baseline period (1990–2019) to a 100 m grid across the NSW using the inverse distance-weighted (IDW) method. We did not use maximum temperature as it was highly correlated with Tmin in the study sites.

We downloaded monthly future projections of Tmin and rainfall generated by 25 GCMs (<https://esgf-node.llnl.gov/search/cmip6/>) (Table 3) from the Coupled Model Intercomparison Project Phase 6 (CMIP6, <https://pcmdi.llnl.gov/CMIP6/>) under different Shared Socio-economic Pathways (SSPs). We selected two SSPs to represent an intermediate “middle of the road” scenario (SSP2-4.5, hereafter referred as SSP245) and a high emissions “fossil-fuelled development” scenario (SSP5-8.5, hereafter referred as SSP585) (O’Neill et al., 2016). Then, these monthly raw gridded future climate data were statistically downscaled to individual climate stations using the method developed by Liu and Zuo (2012). We used IDW method to interpolate annual average of Tmin and rainfall for 25 GCMs in the baseline (1990–2019), 2050s (2031–2060), and 2090s (2071–2100) from 2096 climate sites to the whole study area at a 100 m grid.

#### 2.3.3. Biota

A land disturbance index (LDI) was used to reflect the intensity of disturbance to ecosystem functions associated with land use at a site. Six levels of LDI were classified according to the Australian Soil and Land Survey Field Handbook. For example, LDI 1 denotes natural ecosystems and LDI 6 represents intensive cropping. Detailed descriptions of each LDI class are given by Gray et al. (2015) (Table S1 in Supplementary

**Table 3**

List of 25 global climate models (GCMs) under SSP245 and SSP585 climate scenarios used in the study.

Model ID	Name of GCM	Abbreviation	Institute ID	Country
01	ACCESS-CM2	AC2	BoM	Australia
02	ACCESS-ESM1-5	AC1	BoM	Australia
03	BCC-CSM2-MR	BC1	BCC	China
04	CIESM	CIE	THU	China
05	FGOALS-g3	FGO	FGOALS	China
06	NESM3	NE1	NUIST	China
07	CanESM5	CE1	CCCMA	Canada
08	CanESM5-CanOE	CE2	CCCMA	Canada
09	CNRM-CM	CN1	CNRM	France
10	CNRM-CM6-1-HR	CN2	CNRM	France
11	CNRM-ESM	CN3	CNRM	France
12	EC-Earth3	EC1	EC-EARTH	Europe
13	EC-Earth3-Veg	EC2	EC-EARTH	Europe
14	GFDL-ESM4	GF1	NOAA GFDL	USA
15	GFDL-CM4	GF2	NOAA GFDL	USA
16	GISS-E2-1-G	GIS	NASA GISS	USA
17	INM-CM4-8	IN1	INM	Russia
18	INM-CM5-0	IN2	INM	Russia
19	IPSL-CM	IP1	IPSL	France
20	MIROC6	MI1	MIROC	Japan
21	MIROC-ES2L	MI2	MIROC	Japan
22	MRI-ESM2-0	MR1	MRI	Japan
23	MPI-ESM1-2-HR	MP1	MPI-M	Germany
24	MPI-ESM1-2-LR	MP2	MPI-M	Germany
25	UKESM1-0-LL	UKE	Met Office	UK

Information). We used LDI based on field site data as a numeric variable for model development. For spatial map development, we used 100 m land use grids sourced from [DPIE \(2020\)](#).

#### 2.3.4. Age

Weathering index was used to infer the degree of weathering of parent materials, regolith, and soil based on airborne gamma-ray spectrometry imagery and the SRTM elevation data ([Wilford, 2012](#)). The spatial layer with a 100 m resolution was downloaded from Geoscience Australia. We used weathering index to reflect the age of the soil ([Gray et al., 2019](#)).

#### 2.3.5. Parent material

Silica index represents classes of silica content (%) and provides the quantitative estimation of the chemical composition of most parent materials. In general, soils with higher silica content parent materials have more quartz and sandier textures. For model development, we used the description of parent material recorded by the soil professional at the time of sampling. For the final map development, a silica map with 100 m resolution was sourced from [Gray et al. \(2016\)](#).

Radiometric potassium (Rad\_k), uranium (Rad\_u) and thorium (Rad\_th) with a resolution of 90 m were downloaded from Geoscience Australia (<https://www.ga.gov.au/scientific-topics/disciplines/geophysics/radiometrics>) ([Minty et al., 2009](#)). They were regridded to 100 m.

### 2.4. Prediction model

We applied MLR and RF as two contrasting DSM techniques to model and map SOC stocks in NSW. MLR is an empirical model commonly used in estimating SOC stock while the RF model is an ensemble learning method by constructing a multitude of decision trees to accommodate complex nonlinear relationships ([Breiman, 2001](#)). Because of its high predictive ability, the RF model has been widely applied to estimate SOC stocks at different spatial scales around the world including in Australia ([Wang et al., 2018a](#)), China ([Zhou et al., 2019](#)), and Brazil ([Gomes et al., 2019](#)).

Given that multicollinearity among predict variables can cause problems when fitting MLR, we used variable inflation factor (VIF) to test the degree of correlation between predictors. We found that all 11 predictors used were statistically independent of each other (VIF < 10, Table S2 in Supplementary Information). Linear correlations between SOC stocks and individual predictors were also derived (Table S3 in Supplementary Information). Note that all covariates except Rad\_u and Rad\_k were significantly ( $p < 0.01$ ) correlated with SOC stock. Although non-significant relationships were detected between SOC and Rad\_u or Rad\_k, they were ranked as important variables in machine learning models ([Gray et al., 2019](#); [Wang et al., 2018a](#)). Therefore, in order to do model comparison, we still included them in our MLR model.

The RF model was implemented with the ‘randomForest’ package ([Liaw and Wiener, 2002](#)) in the R software ([R-Core-Team, 2020](#)). The parameters in the RF model were set with mtry (the number of randomly selected predictor variables at each node) of 4 (the number of predictor variables divided by 3) and ntree (the number of trees to grow in the forest) of 1000 ([Ließ et al., 2016](#)). The relative importance of variables was estimated with the training dataset using the “%IncMSE” metric from the RF model. The %IncMSE indicates the mean increase of mean square error in nodes that use a variable in the RF model, when values of the variable are randomly permuted.

We randomly selected 80 % of 2153 soil data for model development and 20 % for validation. This calibration and validation procedure were repeated with 10 bootstraps applying a sampling with replacement method, to obtain 10 random subsamples of the data, each one with its own calibration and validation dataset.

The state-wide maps of SOC stock under current conditions were based on these 10 bootstrap runs. The average of the 10 SOC stock maps was used as final prediction for each DSM technique. We used this

average map as a benchmark of current SOC stocks for NSW. We hypothesized that the complex relationship between SOC and its drivers is time independent ([Yigini and Panagos, 2016](#)). Thus, to project SOC stock in the 2050s and 2090s as impacted by climate change, the prediction model was rerun for NSW using the same spatial layers except for temperature and rainfall from the 25 GCMs under two emission scenarios ([Adhikari et al., 2019](#)). Finally, we calculated the relative change between the baseline and future SOC stock based on GCM projected climate data and assessed the contribution of future climate change to SOC stocks in the study area. All spatial maps under future climate were the average of 10 bootstrap runs.

### 2.5. Model evaluation

To evaluate the goodness of fit measures, we used the coefficients of determination ( $R^2$ , the amount of variation explained by the model) and Lin’s Concordance Correlation Coefficient (LCCC) ([Lin, 1989](#)).  $R^2$  close to 1 indicates a perfect model, i.e. 100 % of variation has been explained by the model. LCCC combines measures of both precision and bias to determine how far the observed data deviate from the 1:1 line, and has been widely used in studies of DSM modelling ([Bonfatti et al., 2016](#); [Malone et al., 2009](#); [Somaratna et al., 2016](#); [Wang et al., 2017](#); [Yang et al., 2016](#); [Zhou et al., 2019](#)). LCCC ranges from -1 to +1 with a value of +1 denoting perfect agreement, values greater than 0.9 showing near perfect agreement, values between 0.8 and 0.9 substantial agreement, between 0.65 and 0.8 moderate agreement, and values < 0.65 poor agreement ([Viscarra Rossel et al., 2014](#)). We also used root mean squared error (RMSE) and mean absolute error (MAE) to measure the difference between values predicted by a model and the values observed. The equations for deriving these four statistical indices are as follows:

$$R^2 = 1 - \frac{SSE}{SST} \quad (2)$$

$$RMSE = \sqrt{\frac{1}{n} \sum_{i=1}^n (P_i - O_i)^2} \quad (3)$$

$$MAE = \frac{1}{n} \sum_{i=1}^n |P_i - O_i| \quad (4)$$

$$LCCC = \frac{2r\sigma_o\sigma_p}{\sigma_o^2 + \sigma_p^2 + (\bar{P} - \bar{O})^2} \quad (5)$$

where SSE is the sum of squared errors at validation points; SST is the total sum of squares;  $P_i$  and  $O_i$  denote the predicted and measured SOC stocks;  $n$  is the number of samples;  $\bar{P}$  and  $\bar{O}$  are the means for the predicted and measured SOC stocks;  $\sigma_o^2$  and  $\sigma_p^2$  are the variances of predicted and observed values and  $r$  is the Pearson correlation coefficient between the predicted and observed values. Models with the higher LCCC and  $R^2$  and lower RMSE and MAE are identified to be the more accurate models.

## 3. Results

### 3.1. Descriptive statistics of SOC stock measurements

The SOC stocks (0–30 cm) of 2153 sampling sites varied from 5.08 to 184.86 t ha<sup>-1</sup>, with a mean value of 46.11 t ha<sup>-1</sup> and a coefficient of variation (CV) of 62.48 % ([Table 4](#)). The observed SOC stocks data were highly positively skewed. Also, there was a high kurtosis value indicating infrequent very high SOC stock values. Both kurtosis and skewness showed that the distribution of original observed SOC stock values was highly non-normal ([Fig. 2a](#)). After the data were log-transformed, the coefficient of skewness and kurtosis became 0.15 and 0.02 respectively indicating the distribution of transformed SOC values was much

**Table 4**

Descriptive statistics of soil organic carbon stock ( $\text{SOC t ha}^{-1}$ ) with original values and natural log-transformed values in the 0–30 cm soil layer in the study area.

	<i>n</i>	Min	Median	Mean	Max	SD	CV (%)	Skewness	Kurtosis
SOC	2153	5.08	37.81	46.11	184.86	28.81	62.48	1.81	4.05
Ln (SOC)	2153	1.62	3.63	3.67	5.22	0.56	15.30	0.15	0.02

Notes: Ln (SOC) is natural log-transformed SOC, *n* is the number of samples, Min is minimum, Max is maximum, SD is standard deviation, CV is coefficient of variation.

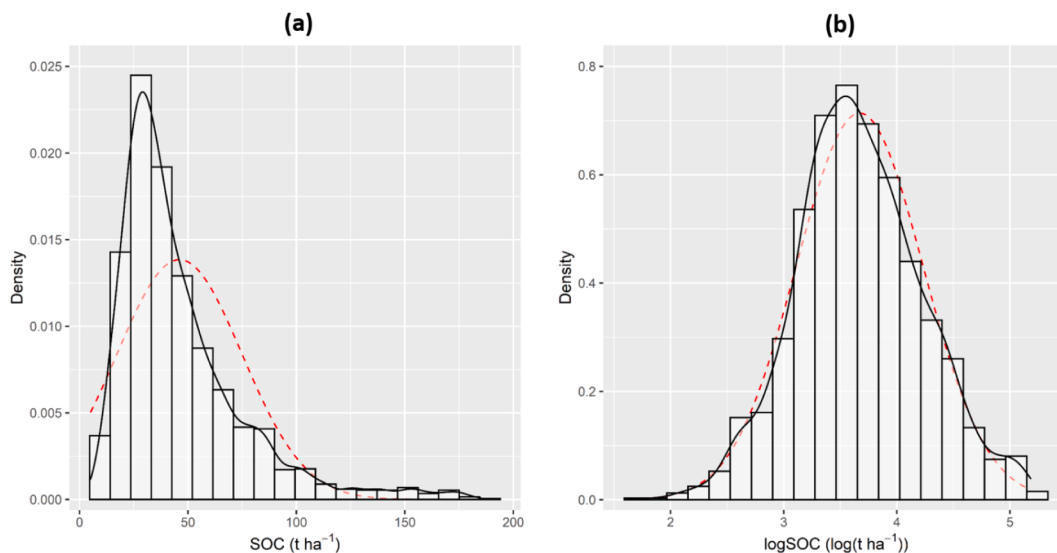


**Fig. 2.** Histograms of soil organic carbon (SOC) stock of 2153 samples from NSW. The black solid curve is the estimated kernel density and the red dashed curve denotes the normal distribution with mean and variance set to those of samples (a) original values; and (b) natural log-transformed values.

closer to normal distribution (Table 4).

### 3.2. Model performance and variable importance

Results of the validation process between the observed and predicted SOC stocks generated by two DSMs (MLR and RF) based on 10 bootstrap runs, using the  $R^2$ , LCCC, RMSE, and MAE, are shown in Table 5. The MLR explained 53 % of the variation of SOC stocks in the validation dataset. The average value of LCCC was 0.68, RMSE was  $19.1 \text{ t ha}^{-1}$ , and MAE was  $13.3 \text{ t ha}^{-1}$ . Overall, the MLR model presented moderate predictive capacity. The average values of  $R^2$  (0.69) and LCCC (0.79) derived from the RF model for the validation data were greater than MLR. Meanwhile, the values of RMSE ( $15.8 \text{ t ha}^{-1}$ ) and MAE ( $10.5 \text{ t ha}^{-1}$ ) in RF were lower compared to MLR. Based on these statistical indices, we found that RF showed greater predictive capacity than MLR in estimating observed SOC stocks.

Fig. 3 summarises the relative importance of 11 predictors in predicting SOC stocks based on 10 runs of RF models. Mean annual rainfall was found to be the most important predictor variable influencing SOC stocks across NSW, followed by Tmin, Rad\_u, LDI, Rad\_th, Silica, and Rad\_k. In contrast, the topographic variables (Slope, TWI, and Aspect) showed a very low contribution to the modelled SOC stocks at this state-wide scale. Based on the regression from the MLR model, we found that SOC stocks had a significantly positive relationship with mean annual rainfall and a significantly negative relationship with minimum temperature (Table 6).

**Table 5**

Model validation results based on the average of 10 bootstrap runs for multiple linear regression (MLR) and random forest (RF) respectively.

Model	$R^2$	LCCC	RMSE ( $\text{t ha}^{-1}$ )	MAE ( $\text{t ha}^{-1}$ )
MLR	0.53	0.68	19.1	13.3
RF	0.69	0.79	15.8	10.5

### 3.3. Spatial prediction of SOC stocks

The state-wide maps of current SOC stocks were based on the average of 10 bootstrap runs, for each DSM technique. Spatially, the estimated SOC stocks increased from the rangelands in western NSW ( $< 25 \text{ t ha}^{-1}$ ), through the mixed farming zone in central NSW and the Tablelands ( $30\text{--}60 \text{ t ha}^{-1}$ ), to coastal areas in eastern NSW (more than  $80 \text{ t ha}^{-1}$ ) for both MLR and RF (Fig. 4). Additionally, we estimated total SOC stocks for each of the 11 LLS regions (Table 7). The total stock of SOC (0–30 cm) ranged from 67.9 to 824.3 Mt across the 11 LLS regions mainly due to differences in climatic conditions, soil type, land use, and the size of LLS regions. For example, the Western LLS region covered the largest area ( $314,493 \text{ km}^2$ ) and had the largest total SOC stock when compared with all other LLS regions despite the lowest mean SOC stock per hectare. The SOC stocks estimated by RF model were slightly higher than MLR model across almost all LLS regions, and the relationship between RF- and MLR-predicted SOC stocks indicated a robust agreement ( $R^2 = 0.99$ ) (Fig. S1 in Supplementary Information).

### 3.4. Projected changes of SOC stocks under future climate

We used MLR only to assess the impacts of climate change on SOC stocks due to some anomalies that resulted from RF, as described in the Discussion. Projected multi-GCM ensemble mean changes in SOC stocks ( $\text{t ha}^{-1}$ ) across NSW for two future periods (2050s and 2090s) under SSP245 and SSP585 scenarios relative to the baseline climate of 1990–2019, based on MLR, are shown in Fig. 5. Also, we presented the projected changes in SOC stocks (%) across 11 LLS regions based on 25 GCMs under different emission scenarios (Fig. 6). SOC stocks were predicted to decrease across NSW with the magnitude of decrease depending on regions and emission scenarios (Fig. 5). For example, a larger decrease in SOC stocks was forecast in the eastern NSW high-rainfall areas including the North Coast, Northern Tablelands, Hunter, and alpine region compared with the low-rainfall area of western NSW.

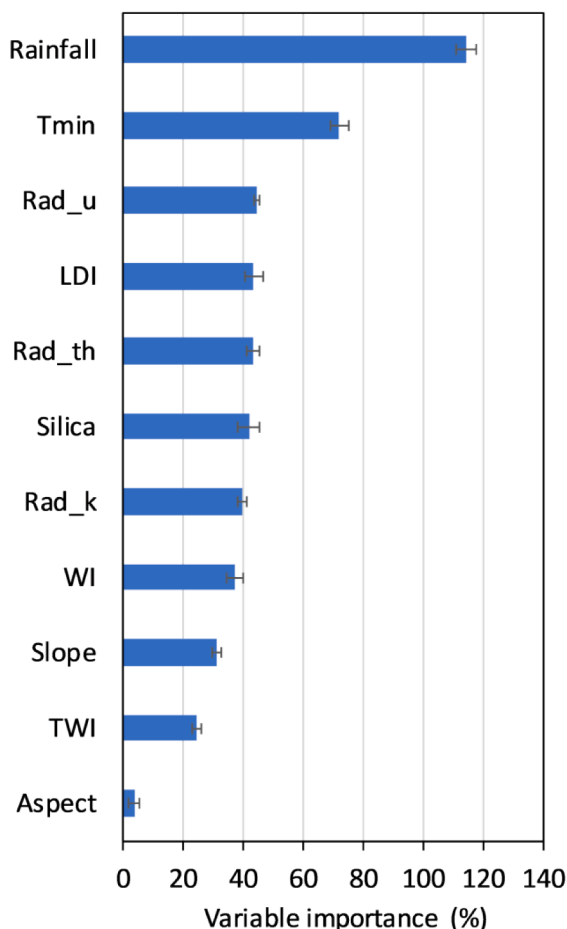


**Fig 3.** Patterns in the importance of each predictor variable used in random forest (RF) to predict SOC stocks for the 0–30 cm soil layer based on 10 runs.

(Fig. 5). As temperature increased most in the 2090s under SSP585, SOC stocks showed the largest decrease under this scenario (Fig. 5d). However, there were large variations in magnitude and direction of change in SOC stocks projected between individual GCMs (Figs. S2–5 in Supplementary Information). As an example, the GF2 model projected decreased SOC stocks over the eastern parts of NSW under SSP585 (Figs. S4 and S5 in Supplementary Information). Conversely, the EC2 displayed an increase in the same regions under SSP585 (Figs. S4 and S5 in Supplementary Information) and an increase was also seen in some parts of the Western region in the 2050s under SSP245 (Fig. S2 in Supplementary Information).

SOC stock change (%) showed a larger variation among the 25 GCMs under SSP585\_2090s for the majority of LLS regions compared to other scenarios (Fig. 6). This is likely explained by changes in rainfall and temperature under a high emission scenario (Figs. S6 and S7 in

**Table 7**

Estimation of SOC stocks in the 0–30 cm soil layer based on RF and MLR for 11 Local Land Service (LLS) regions in NSW.

LLS regions	Area (km <sup>2</sup> )	RF		MLR	
		SOC stocks (t ha <sup>-1</sup> )	Total SOC stocks (Mt)	SOC stocks (t ha <sup>-1</sup> )	Total SOC stocks (Mt)
Central Tablelands	31,347	53.7	168.2	51.3	160.7
Hunter	33,006	68.3	225.3	55.5	183.3
North Coast	32,060	84.1	269.5	81.8	262.2
Northern Tablelands	39,509	54.6	215.7	55.4	218.9
South East	55,627	59.0	328.4	59.0	328.4
Western	314,493	26.2	824.3	22.7	712.4
Riverina	67,083	39.9	267.4	35.4	237.7
Murray	41,899	41.7	174.6	39.9	167.3
Greater Sydney	12,497	64.1	80.2	54.3	67.9
Central West	91,619	38.9	356.6	33.4	306.2
North West	82,443	39.5	326.0	36.3	299.4
NSW	801,583	40.4	3236.2	36.7	2944.5

**Table 6**

Regression coefficient of SOC stocks (log) with 11 predictors in MLR. \*p < 0.05, \*\*p < 0.01.

	Slope	TWI	Aspect	Rad_k	Rad_th	Rad_u	Silica	WI	LDI	Tmin	Rain
Regression coefficient	-0.005	-0.043**	0.015	-0.004	-0.008*	0.018	-0.011**	0.05*	-0.05**	-0.053**	0.001**

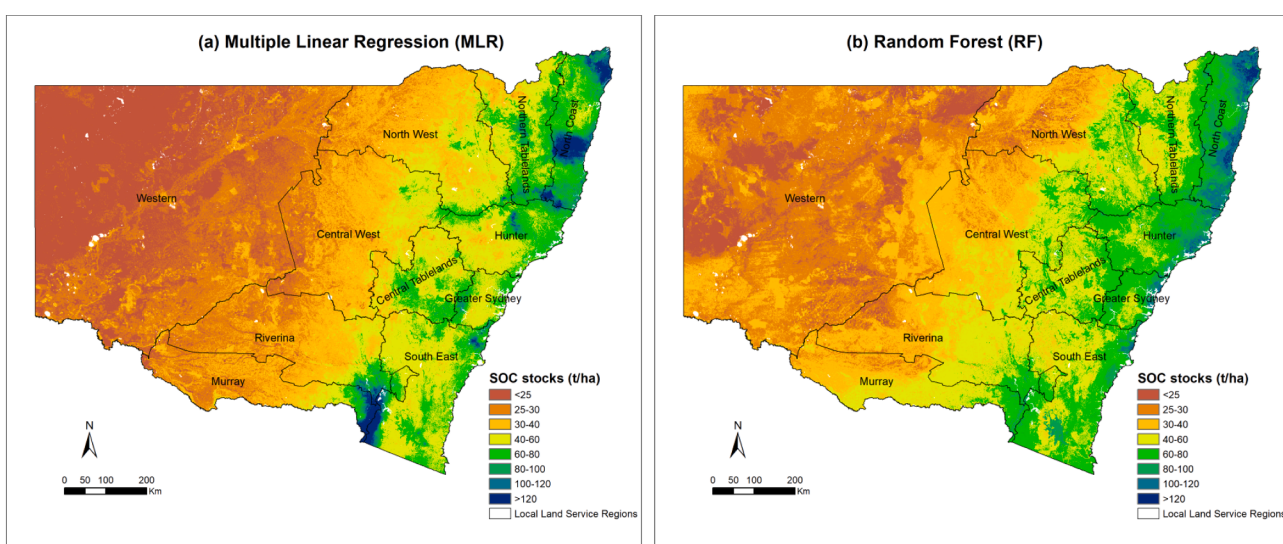


**Fig 4.** Spatial distribution of current SOC stocks (0–30 cm) estimated by MLR and RF.

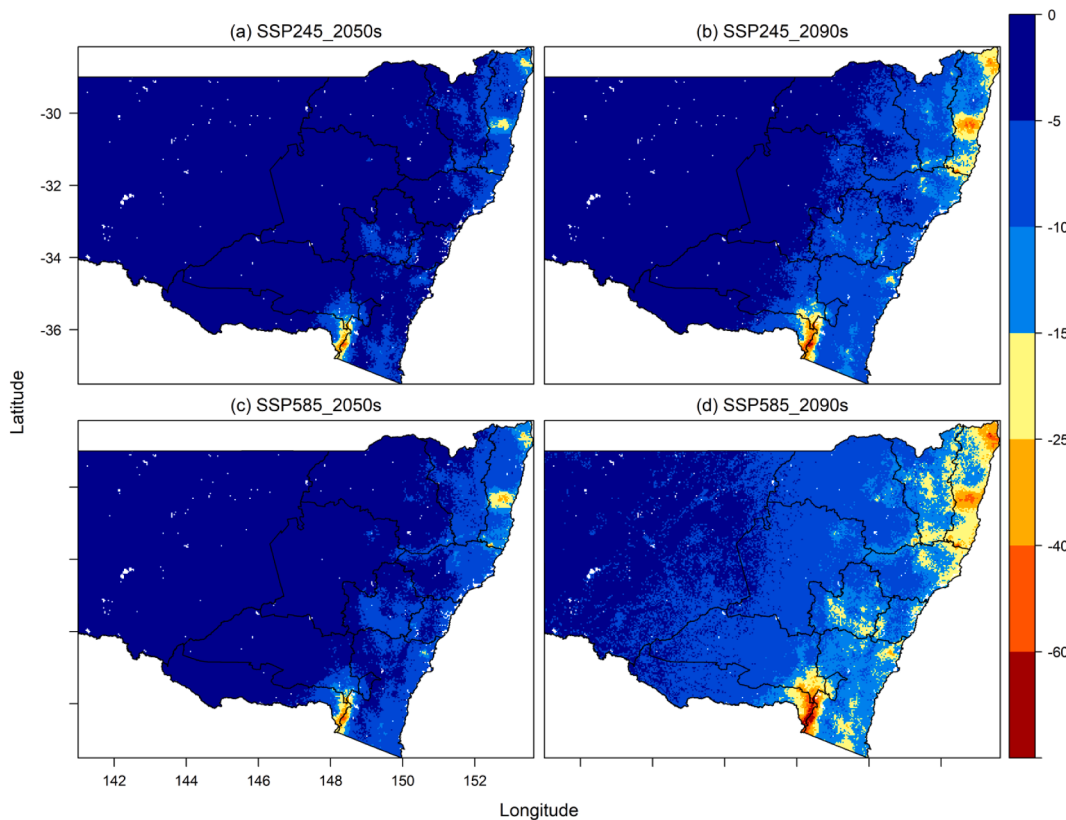


**Fig 5.** Multi-GCM ensemble mean change in SOC stocks ( $t\text{ ha}^{-1}$ ) in the 2050s and 2090s under different emission scenarios (SSP245 and SSP585) compared to the baseline (1990–2019) based on MLR.

**Supplementary Information).** For example, the range of 10th (Q10) and 90th (Q90) percentiles of the boxplot for Western region was 10 % in the 2050s under SSP245. By contrast, the range of Q10–Q90 reached 17 % in the 2090s under SSP585. Also, we noted that there was a higher variability in SOC stocks change in higher rainfall LLS regions; that is, increasing dispersion between Q90 and Q10 (Fig. 6). For example, the range of Q10–Q90 for SOC stock changes under SSP585\_2090s was 46 % in the North Coast region (high-rainfall LLS region) and 24 % in the North West region (low-rainfall LLS region).

Further, we analysed the change in SOC stocks (%) for different LLS regions in response to annual rainfall change and Tmin change (Table 8). Overall, changes in rainfall and Tmin projected by 25 GCMs under two emission scenarios explained 76–99 % of the variation in SOC change (percentage change in SOC stock). Relative changes in rainfall (%) had a larger influence on SOC change in high rainfall LLS regions (e.g. North Coast, Northern Tablelands, and South East) than in low rainfall regions (e.g. Western), which indicates that change in rainfall was a stronger driver of SOC change in wetter regions than drier regions. In contrast, there was a negative relationship between SOC stocks and Tmin (Table 8). Additionally, the relative change in SOC stocks was more sensitive to Tmin change in high-rainfall LLS regions (e.g. Greater Sydney and South East) than that in low-rainfall LLS regions (e.g. Western).

#### 4. Discussion

In this study, we validated the performance of both MLR and RF model in estimating SOC stocks. We demonstrated the ability of these two DSM techniques in predicting soil carbon storage based on different environmental covariates across NSW. The performance of SOC models developed in our study appears broadly comparable with previous studies. For example, the statistical metrics obtained by each model

were similar to those obtained by Gray and Bishop (2019), who used MLR to project the change in SOC stock with 12 climate models in southeast Australia. Their model had a mean LCCC of 0.59. Our results are also consistent with Viscarra Rossel et al. (2014) who used decision models to estimate SOC stocks with values of LCCC ranging from 0.75 to 0.82. Similarly, we identified that the most important predictors determining SOC at regional scales are climatic factors, specifically rainfall and temperature. Given these results, we were confident to apply these models in subsequent analysis on the impacts of future climate on SOC stocks.

When we applied RF to predict effects of climate change on SOC stocks, there were some anomalies that arose with such decision tree models. For example, in some regions the projected SOC stock would increase when rainfall decreased and temperature increased, the opposite to normal expected trends. Previous studies have also identified similar issues in the application of decision tree models to predict SOC stock change (Gray and Bishop, 2019). RF revealed a limitation in handling covariate shift when we changed temperature and rainfall under future climate scenarios but assumed the relationship between SOC and other predictors remained constant. In other words, the RF modelling technique did not appear to be reliable or suitable for use in this ‘space-for-time substitution’ modelling process (Gray and Bishop, 2019; Quinonero-Candela et al., 2009). This apparent weakness in decision tree models needs further examination. Due to this weakness, we only used MLR to assess the impacts of climate change on SOC stocks in NSW. We included the RF model results for current SOC stocks because the model performed well, as indicated by the statistics presented, and the issues with covariate shift do not apply to the baseline assessment. The strong agreement between our MLR model and RF model in predicting SOC stocks over LLS regions ( $R^2 = 0.99$ , Fig. S1 in Supplementary Information) provides confidence in the use of the MLR model to predict the change in SOC stocks under climate change.



**Fig 6.** Projected changes in SOC stocks (%) in the 2050s and 2090s under SSP245 and SSP585 compared with the baseline (1990–2019) for each LLS region in the NSW, based on MLR. Box boundaries indicate the 25th and 75th percentiles across 25 GCMs, and whiskers below and above the box indicate the 10th and 90th percentiles. The black lines and crosshairs within each box indicate the multi-model median and mean, respectively.

**Table 8**

Regression coefficients of changes in SOC stocks ( $\Delta\text{SOC}$ , %) with changes in annual mean minimum temperature ( $\Delta\text{Tmin}$ ,  $^{\circ}\text{C}$ ) and rainfall ( $\Delta\text{Rain}$ , %) in a linear regression model ( $\Delta\text{SOC} = a \cdot \Delta\text{Tmin} + b \cdot \Delta\text{Rain} + c$ ) for 11 Local Land Service (LLS) regions in NSW. All correlation coefficients are significant ( $p < 0.001$ ).

LLS regions	a	b	$R^2$
Central Tablelands	-5.00	0.83	0.95
Hunter	-5.19	1.02	0.88
North Coast	-5.06	1.49	0.87
Northern Tablelands	-4.80	0.93	0.94
South East	-5.22	0.88	0.86
Western	-4.66	0.30	0.99
Riverina	-4.86	0.57	0.97
Murray	-4.87	0.65	0.96
Greater Sydney	-5.66	1.00	0.76
Central West	-4.88	0.56	0.96
North West	-4.95	0.65	0.93

We found that future climate change would have negative impacts on SOC stocks in the surface soil layer (0–30 cm). Generally, SOC stocks will decline across NSW with the largest decline occurring in the North Coast and South East alpine regions where current SOC stocks are high. The magnitude of the projected decline in SOC stocks across NSW was greatest in the 2090s under a high emission scenario SSP585, with a marked change in climate relative to the baseline. The general decline in SOC stocks projected in our study is consistent with a previous study in Australia (Gray and Bishop, 2019). However, it is critical to recognise differences in values of projected SOC stock change because different observed data (including soil variables other than SOC), predictor

variables, climate data, and DSM techniques were used. For example, Gray and Bishop (2019) used MLR model to simulate changes in SOC stocks in southeast Australia based on 12 climate models representing four GCMs downscaled with three regional models and sourced from the NSW and ACT Regional Climate Modelling project (Evans et al., 2014). They reported a region-wide average decrease in SOC stocks of  $1.7 \text{ t ha}^{-1}$  in the 0–30 cm soil layer for the near-future change period (centred around 2030) and  $4.0 \text{ t ha}^{-1}$  to the far-future change period (centred around 2070) based on the average of all climate models. Similarly, Reyes Rojas et al. (2018) predicted that SOC stocks in central Chile will decrease by 9.7 % under RCP4.5 and 12.9 % under RCP8.5 by the year 2050. There is agreement among studies that where the high emission scenarios are used as climate projection inputs to statistical models, a decline in SOC stocks is more likely (Gollany and Venterea, 2018). In addition, our findings agree with the aforementioned studies that soils with higher SOC stocks will incur a greater proportional decrease in SOC compared to those with lower SOC stocks (Gray and Bishop, 2019; Reyes Rojas et al., 2018). Furthermore, we found that the relative change of SOC stocks was more sensitive to  $\text{Tmin}$  and rainfall change in high rainfall regions (e.g. Greater Sydney) than that in low-rainfall LLS regions (e.g. Western) (Table 8). This is because these low rainfall areas are already warm and dry where current SOC stocks are low, so changing temperature and rainfall will have limiting effects on SOC (Gibson et al., 2021; Hoyle et al., 2016).

The 25 GCMs was used in this study to consider the variance of climate projections. The use of many GCMs is key to capturing the variability in future projections related to uncertainties in model structure and parameterization (Wang et al., 2018b). Rainfall in Australia is highly variable. Therefore, rainfall projections are less

robust and present larger variance than temperature projections. Here, we used multi-GCM ensemble means to quantify the magnitude of future SOC stock changes to provide a robust assessment of climate change impact on SOC stocks in NSW.

Similar to previous studies (Adhikari et al., 2019; Reyes Rojas et al., 2018), we used empirical modelling to estimate SOC stocks with 11 different environmental covariates based on multiple datasets and then applied the relationship to spatial soil databases to obtain regional estimates for future climate. Bui et al. (2009) and Hobley et al. (2015) found strong regionalization of SOC levels with annual mean moisture index and vapour pressure deficit for eastern Australia. However, we did not include these climate variables in our model since they are not available for future projections.

We substituted the historical temperature and rainfall in the regression model with GCM projected temperature and rainfall while keeping other environmental variables constant over time to model SOC change (Reyes Rojas et al., 2018; Yigini and Panagos, 2016). The limitation of a substitution of rainfall and temperature is that we ignore the change in other covariates. One of the predictors most likely to change is land use related to human activities. Land use adaptation should be considered as a response to mitigate the negative impact of climate change on SOC (Minasny et al., 2017). Note that land managers may reduce the intensity of soil disturbance associated with the land use. For example, changing from cropping to native and improved pasture can achieve an average SOC sequestration rate of  $1.2 \text{ t ha}^{-1}$  per year in central west of NSW (Badgery et al., 2021).

Luo et al. (2017) reported that the direct contribution of climate to SOC change rate is comparable to other variables, such as initial SOC stock and pools, C inputs, and soil properties, across Australian cropping systems. This is because climate plays a key role in regulating plant growth thus potential C input to the soil, as well as microbial activity and therefore OM decomposition. This role can be moderated by agronomic practices such as changing cropping systems and rotations, fertilizer and residue management, and tillage, all of which influence C inputs microbial activity and the soil environment (Luo et al., 2017). By using process-based carbon models, previous studies found that changes in SOC stocks were more pronounced between management practices such as crop rotations and soil tillage than different climate change scenarios (Farina et al., 2011; Lugato and Berti, 2008). However, these conclusions may not be applicable to different study regions. We did not consider the impact of agricultural management practices on SOC sequestration. Compared with DSM techniques, biophysical process-based carbon models such as Century and RothC have higher capability to simulate the interactive effects of climate and soil management within and between regions (Caddeo et al., 2019; Gottschalk et al., 2012; Liu et al., 2009; Luo et al., 2019).

Climate change is expected to have significant effects on SOC stocks, mainly through the impact of changes in soil moisture, temperature, and CO<sub>2</sub> levels on plant growth and biogeochemical processes (Lal, 2004). Elevated atmospheric CO<sub>2</sub> concentrations generally increase the inputs of readily assimilated carbon compounds to soils through greater leaf and root production and enhanced root exudation (Sulman et al., 2014). The turnover of SOC is closely linked to belowground C supply from plant roots in the form of root exudates. However, the turnover rate may be moderated by lower soil water and increased temperatures under future climate scenarios.

There is some uncertainty in projecting SOC stock under different climate scenarios. First, the direction and magnitude of SOC change are largely dependent on the climate model and emission scenario used. For example, under the high emission scenario SSP585, a large SOC decrease can be found for the CN1 model in the 2090s (Fig. S5 in Supplementary Information). Significant range of projected SOC change (Q10–Q90) is demonstrated for each LLS region in the 2090s under SSP585 (Fig. 6). Climate projection is a major source of uncertainty in modelling the impacts of climate change on SOC. Therefore, with more certainty and reliability in projecting future climates especially for rainfall, we will be

able to more confidently predict SOC change under future climate. Second, a weakness of our modelling process is its failure to capture complex interactions between soil and atmospheric CO<sub>2</sub> levels, vegetation growth, and a changing climate (Gray and Bishop, 2019). This may conceivably overestimate the negative impacts of decreased rainfall and increased temperature on SOC as the associated feedback mechanisms between soil and vegetation under elevated CO<sub>2</sub> concentration were not considered.

Understanding and predicting the way SOC stocks will respond to climate change in different regions is important to support land use planning and climate policy (Caddeo et al., 2019). We found that SOC decline is more marked under future climate scenarios in eastern parts of NSW where current SOC stocks are high compared with the western region where SOC stocks are relatively low. This is mainly due to more increased temperature occurring in most eastern areas of NSW (Fig. S6 in Supplementary Information). Our study has assessed the impacts of future climate on total SOC stocks, but it is important to note that the composition of the SOC pool (that is, the amount of particulate OC, mineral-associated OC, and char) will influence its vulnerability to decomposition with changes in rainfall and temperature (Krull et al., 2003). We expect the information provided in this study can be used to identify areas where targeted land management interventions are needed to maintain current SOC stocks or slow the forecast decline in SOC stocks. Previous studies have suggested several management practices to increase the SOC stocks in rainfed agricultural areas of NSW (Conyers et al., 2015; Liu et al., 2016). Practices such as introducing cover crops, changing crop and pasture sequence, including a legume phase and nutrient management can increase SOC sequestration, slow SOC decline, and help to overcome the impacts of drought under projected climate change scenarios (Liu et al., 2014; Liu et al., 2016). For example, including a pasture phase with legumes that have a lower soil-water requirement than cereal crops can simultaneously support biological nitrogen fixation, improve soil structure and increase the rate of SOC accumulation (Wu et al., 2017). Therefore, different agronomic management options should be investigated in different LLS regions to identify the potential for SOC management to contribute to climate change mitigation in the future.

## 5. Conclusions

We used DSM techniques to predict the SOC stock (0–30 cm) changes for NSW under SSP245 and SSP585 in the 2050s and 2090s. The 25 GCMs were used to represent possible future climate projections. This is the first study in Australia that used multiple GCMs in the CMIP6 ensemble to understand how anticipated climate change will affect our vital soil resources at the State scale. We found that:

- The current SOC stocks in NSW averaged from  $36.7 \text{ t ha}^{-1}$  for MLR to  $40.4 \text{ t ha}^{-1}$  for RF and decreased from east to west.
- The most important predictors of SOC stocks in NSW were rainfall and minimum temperature.
- Multi-GCM ensemble means allowed the identification of natural resource management regions that would experience the greatest decline in SOC stocks under future climate change.
- There was a decrease in SOC stocks in all scenarios, but the scenario with higher radiative forcing (SSP585) resulted in the largest decline in SOC stocks by the end of 21st century.

Projections of SOC stocks for the different LLS regions obtained in our research can be used as a basis for identifying areas susceptible to SOC decline as a consequence of climate change across the state of NSW. Combining DSM with spatial databases enabled assessment of changes in regional SOC stocks to inform land management and climate change strategies and policies. The significant decline in SOC stocks projected even under moderate climate change highlights the potential risks to landholders of engaging in carbon trading, and the expected challenges

for jurisdictions targeting net zero greenhouse gas emissions. Moreover, our methodology is easily transferrable to other regions where information on edaphic and landscape properties, land use, and climate data are available.

## Declaration of Competing Interest

The authors declare that they have no known competing financial interests or personal relationships that could have appeared to influence the work reported in this paper.

## Acknowledgement

This study was funded by the NSW Primary Industries Climate Change Research Strategy and the NSW Climate Change Fund. We acknowledge the World Climate Research Programme, which, through its Working Group on Coupled Modelling, coordinated and promoted CMIP6. We thank the climate modelling groups for producing and making available their model output, the Earth System Grid Federation (ESGF) for archiving the data and providing access, and the multiple funding agencies who support CMIP6 and ESGF. We thank Dr Bernie Dominiak for his review to improve an early version of the manuscript. We also thank anonymous reviewers and editor for their detailed and constructive comments.

## Appendix A. Supplementary data

Supplementary data to this article can be found online at <https://doi.org/10.1016/j.geoderma.2021.115442>.

## References

- ABARES Catchment Scale Land Use of Australia - Update December 2020 Australian Bureau of Agricultural and Resource Economics and Sciences, Canberra, February, CC BY 4 2021 10.25814/ajqjw-rq15.
- Adhikari, K., Owens, P.R., Libohova, Z., Miller, D.M., Wills, S.A., Nemecek, J., 2019. Assessing soil organic carbon stock of Wisconsin, USA and its fate under future land use and climate change. *Sci. Total Environ.* 667, 833–845.
- Badgery, W., Murphy, B., Cowie, A., Orgill, S., Rawson, A., Simmons, A., Crean, J., 2021. Soil carbon market-based instrument pilot – the sequestration of soil organic carbon for the purpose of obtaining carbon credits. *Soil Res.* 59 (1), 12. <https://doi.org/10.1071/SR19331>.
- Bennett, L.T., Hinko-Najera, N., Aponte, C., Nitschke, C.R., Fairman, T.A., Fedrigo, M., Kasel, S., 2020. Refining benchmarks for soil organic carbon in Australia's temperate forests. *Geoderma* 368, 114246. <https://doi.org/10.1016/j.geoderma.2020.114246>.
- Bioregions NSW. 2021. The Bioregions of New South Wales, <https://www.environment.nsw.gov.au/topics/animals-and-plants/biodiversity/bioregions/bioregions-of-nsw>.
- Bonfatti, B.R., Hartemink, A.E., Giasson, E., Tornquist, C.G., Adhikari, K., 2016. Digital mapping of soil carbon in a viticultural region of Southern Brazil. *Geoderma* 261, 204–221.
- L. Breiman Random forests. Machine learning 45 2001 5 32.
- Bui, E., Henderson, B., Viergever, K., 2009. Using knowledge discovery with data mining from the Australian Soil Resource Information System database to inform soil carbon mapping in Australia. *Global Biogeochem. Cycles* 23 (4), n/a–n/a.
- Caddeo, A., Marras, S., Sallustio, L., Spano, D., Sirca, C., 2019. Soil organic carbon in Italian forests and agroecosystems: Estimating current stock and future changes with a spatial modelling approach. *Agric. For. Meteorol.* 278, 107654. <https://doi.org/10.1016/j.agrformet.2019.107654>.
- Cannon, A.J., 2020. Reductions in daily continental-scale atmospheric circulation biases between generations of global climate models: CMIP5 to CMIP6. *Environ. Res. Lett.* 15 (6), 064006. <https://doi.org/10.1088/1748-9326/ab7e4f>.
- Conyers, M., Liu, D.L., Kirkegaard, J., Orgill, S., Oates, A., Li, G., Poile, G., Kirkby, C., 2015. A review of organic carbon accumulation in soils within the agricultural context of southern New South Wales, Australia. *Field Crops Research* 184, 177–182.
- CSIRO, BoM, Climate Change in Australia Information for Australia's Natural Resource Management Regions: Technical Report 2015 CSIRO and Bureau of Meteorology Australia.
- Dane JH, Topp CG. 2002. Methods of soil analysis: Part 4 Physical Methods. In: Agronomy no. 9. Soil Science Society of America: Madison, Wis. USA.
- DPIE. 2020. NSW Landuse 2017. NSW Department of Planning Industry and Environment, <https://datasets.seed.nsw.gov.au/dataset/nsw-landuse-2017-v1p2-foed> (accessed 28.8.2020).
- J. P. Evans F. Ji C. Lee P. Smith D. Argüeso L. Fita Design of a regional climate modelling projection ensemble experiment—NARClIM Geoscientific Model Development 7 2 2014 621 629.
- Farina, Roberta, Seddaiu, Giovanna, Orsini, Roberto, Steglich, Evelyn, Roggero, Pier Paolo, Francaviglia, Rosa, 2011. Soil carbon dynamics and crop productivity as influenced by climate change in a rainfed cereal system under contrasting tillage using EPIC. *Soil Tillage Res.* 112 (1), 36–46.
- Feng, Puyu, Liu, De Li, Wang, Bin, Waters, Cathy, Zhang, Mingxi, Yu, Qiang, 2019. Projected changes in drought across the wheat belt of southeastern Australia using a downscaled climate ensemble. *Int. J. Climatol.* 39 (2), 1041–1053.
- Gerald Forkuor Ozias K. L. Hounkpatin Gerhard Welp Michael Thiel Dafeng Hui High Resolution Mapping of Soil Properties Using Remote Sensing Variables in South-Western Burkina Faso: A Comparison of Machine Learning and Multiple Linear Regression Models PLOS ONE 12 1 2017 e0170478. 10.1371/journal.pone.0170478. s003.
- Gallant, John C., Austin, Jenet M., 2015. Derivation of terrain covariates for digital soil mapping in Australia. *Soil Res.* 53 (8), 895. <https://doi.org/10.1071/SR14271>.
- J.C. Gallant J.P. Wilson Primary topographic attributes, chapter 3 . in Wilson, J.P. and Gallant, J.C. Terrain Analysis: Principles and Applications 2000 John Wiley & Sons.
- Gibson, A.J., Hancock, G.R., Verdon-Kidd, D.C., Martinez, C., Wells, T., 2021. The impact of shifting Köppen-Geiger climate zones on soil organic carbon concentrations in Australian grasslands. *Global Planet. Change* 202, 103523. <https://doi.org/10.1016/j.gloplacha.2021.103523>.
- Gollany, Hero T., Venterea, Rodney T., 2018. Measurements and Models to Identify Agroecosystem Practices That Enhance Soil Organic Carbon under Changing Climate. *J. Environ. Qual.* 47 (4), 579–587.
- Gomes, Lucas Carvalho, Faria, Raiza Moniz, de Souza, Eliana, Veloso, Gustavo Vieira, Schaefer, Carlos Ernesto G.R., Filho, Elpidio Inácio Fernandes, 2019. Modelling and mapping soil organic carbon stocks in Brazil. *Geoderma* 340, 337–350.
- P. Gottschalk J.U. Smith M. Wattenbach J. Bellarby E. Stehfest N. Arnell T. J. Osborn C. Jones P. Smith How will organic carbon stocks in mineral soils evolve under future climate? Global projections using RothC for a range of climate change scenarios *Biogeosciences* 9 8 2012 3151 3171.
- Gray, Jonathan, Karunarathne, Senani, Bishop, Thomas, Wilson, Brian, Veeragathipillai, Manoharan, 2019. Driving factors of soil organic carbon fractions over New South Wales, Australia. *Geoderma* 353, 213–226.
- J.M. Gray T.F.A. Bishop Mapping change in key soil properties due to climate change over south-eastern Australia *Soil Research* 57 2019 805 805.
- Gray, Jonathan M., Bishop, Thomas F.A., Wilford, John R., 2016. Lithology and soil relationships for soil modelling and mapping. *CATENA* 147, 429–440.
- Jonathan M. Gray Thomas F. A. Bishop Xihua Yang Pragmatic models for the prediction and digital mapping of soil properties in eastern Australia *Soil Research* 53 1 2015 24 10.1071/SR13306.
- Grimm, R., Behrens, T., Märker, M., Elsenbeer, H., 2008. Soil organic carbon concentrations and stocks on Barro Colorado Island — Digital soil mapping using Random Forests analysis. *Geoderma* 146 (1-2), 102–113.
- Guerszman, Juan P., Scarth, Peter F., McVicar, Tim R., Renzullo, Luigi J., Malthus, Tim J., Stewart, Jane B., Rickards, Jasmine E., Trevithick, Rebecca, 2015. Assessing the effects of site heterogeneity and soil properties when unmixing photosynthetic vegetation, non-photosynthetic vegetation and bare soil fractions from Landsat and MODIS data. *Remote Sens. Environ.* 161, 12–26.
- Hobley, Eleanor, Wilson, Brian, Wilkie, Arjan, Gray, Jonathan, Koen, Terry, 2015. Drivers of soil organic carbon storage and vertical distribution in Eastern Australia. *Plant Soil* 390 (1-2), 111–127.
- Hoyle, F.C., O'Leary, R.A., Murphy, D.V., 2016. Spatially governed climate factors dominate management in determining the quantity and distribution of soil organic carbon in dryland agricultural systems. *Sci. Rep.* 6, 31468.
- Jeffrey, Stephen J., Carter, John O., Moodie, Keith B., Beswick, Alan R., 2001. Using spatial interpolation to construct a comprehensive archive of Australian climate data. *Environ. Modell. Software* 16 (4), 309–330.
- Reto Knutti The end of model democracy? *Climatic Change* 102 3-4 2010 395 404.
- Krull, Evelyn S., Baldock, Jeffrey A., Skjemstad, Jan O., 2003. Importance of mechanisms and processes of the stabilisation of soil organic matter for modelling carbon turnover. *Funct. Plant Biol.* 30 (2), 207. <https://doi.org/10.1071/FP02085>.
- Lal, R., 2004. Soil Carbon Sequestration Impacts on Global Climate Change and Food Security. *Science* 304 (5677), 1623–1627.
- Liaw, A., Wiener, M., 2002. Classification and regression by randomForest. *R news*, 2, 18–22.
- Ließ, Mareike, Schmidt, Johannes, Glaser, Bruno, Ebrahimi, Mansour, 2016. Improving the Spatial Prediction of Soil Organic Carbon Stocks in a Complex Tropical Mountain Landscape by Methodological Specifications in Machine Learning Approaches. *PLoS ONE* 11 (4), e0153673. <https://doi.org/10.1371/journal.pone.0153673>. [https://doi.org/10.1371/journal.pone.0153673](https://doi.org/10.1371/journal.pone.0153673.g00110.1371/journal.pone.0153673.g00210.1371/journal.pone.0153673.g00310.1371/journal.pone.0153673.g00410.1371/journal.pone.0153673.g00510.1371/journal.pone.0153673.t00110.1371/journal.pone.0153673.t00210.1371/journal.pone.0153673.t00310.1371/journal.pone.0153673.t004).
- Lin, Lawrence I-Kuei, 1989. A Concordance Correlation Coefficient to Evaluate Reproducibility. *Biometrics* 45 (1), 255. <https://doi.org/10.2307/2532051>.
- Liu, De Li, Anwar, Muhuddin R., O'Leary, Garry, Conyers, Mark K., 2014. Managing wheat stubble as an effective approach to sequester soil carbon in a semi-arid environment: Spatial modelling. *Geoderma* 214-215, 50–61.
- Liu, De Li, Chan, K. Yin, Conyers, Mark K., 2009. Simulation of soil organic carbon under different tillage and stubble management practices using the Rothamsted carbon model. *Soil Tillage Res.* 104 (1), 65–73.
- Liu, De Li, O'Leary, Garry J., Ma, Yuchun, Cowie, Annette, Li, Frank Yonghong, McCaskill, Malcolm, Conyers, Mark, Dalal, Ram, Robertson, Fiona, Dougherty, Warwick, 2016. Modelling soil organic carbon 2. Changes under a range

- of cropping and grazing farming systems in eastern Australia. *Geoderma* 265, 164–175.
- Liu, D.L., Zuo, H., 2012. Statistical downscaling of daily climate variables for climate change impact assessment over New South Wales, Australia. *Climatic Change* 115, 629–666.
- Lobell, David B., Hammer, Graeme L., Chenu, Karine, Zheng, Bangyou, McLean, Greg, Chapman, Scott C., 2015. The shifting influence of drought and heat stress for crops in Northeast Australia. *Glob. Change Biol.* 21 (11), 4115–4127.
- Lozano-García, Beatriz, Muñoz-Rojas, Miriam, Parras-Alcántara, Luis, 2017. Climate and land use changes effects on soil organic carbon stocks in a Mediterranean semi-natural area. *Sci. Total Environ.* 579, 1249–1259.
- Lucht, W., Schaphoff, S., Erbrecht, T., Heyder, U., Cramer, W., 2006. Terrestrial vegetation redistribution and carbon balance under climate change. *Carbon Balance Manage.* 1, 6.
- Lugato, E., Berti, A., 2008. Potential carbon sequestration in a cultivated soil under different climate change scenarios: A modelling approach for evaluating promising management practices in north-east Italy. *Agric. Ecosyst. Environ.* 128 (1–2), 97–103.
- Luo, Zhongkui, Eady, Sandra, Sharma, Bharat, Grant, Timothy, Liu, De Li, Cowie, Annette, Farquharson, Ryan, Simmons, Aaron, Crawford, Debbie, Searle, Ross, Moore, Andrew, 2019. Mapping future soil carbon change and its uncertainty in croplands using simple surrogates of a complex farming system model. *Geoderma* 337, 311–321.
- Luo, Zhongkui, Feng, Wenting, Luo, Yiqi, Baldock, Jeff, Wang, Enli, 2017. Soil organic carbon dynamics jointly controlled by climate, carbon inputs, soil properties and soil carbon fractions. *Glob. Change Biol.* 23 (10), 4430–4439.
- Malone, B.P., McBratney, A.B., Minasny, B., Laslett, G.M., 2009. Mapping continuous depth functions of soil carbon storage and available water capacity. *Geoderma* 154 (1–2), 138–152.
- McBratney, A.B., Mendonça Santos, M.L., Minasny, B., 2003. On digital soil mapping. *Geoderma* 117 (1–2), 3–52.
- Budiman Minasny Brendan P. Malone Alex B. McBratney Denis A. Angers Dominique Arrouays Adam Chambers Vincent Chaplot Zueng-Sang Chen Kun Cheng Bhabani S. Das Damien J. Field Alessandro Gimona Carolyn B. Hedley Suk Young Hong Biswapati Mandal Ben P. Marchant Manuel Martin Brian G. McConkey Vera Leatitia Mulder Sharon O'Rourke Anne C. Richer-de-Forges Inakwu Odeh José Padarian Keith Paustian Genxing Pan Laura Poggio Igor Savin Vladimir Stolbovoy Uta Stockmann Yiyi Sulaiman Chun-Chih Tsui Tor-Gunnar Vägen Bas van Wesemael Leigh Winowiecki Soil carbon 4 per mille Geoderma 292 2017 59 86.
- Minty, Brian, Franklin, Ross, Milligan, Peter, Richardson, Murray, Wilford, John, 2009. The Radiometric Map of Australia. *Explor. Geophys.* 40 (4), 325–333.
- O'Neill, Brian C., Tebaldi, Claudia, van Vuuren, Detlef P., Eyring, Veronika, Friedlingstein, Pierre, Hurtt, George, Knutti, Reto, Kriegler, Elmar, Lamarque, Jean-François, Lowe, Jason, Meehl, Gerald A., Moss, Richard, Riahi, Keywan, Sanderson, Benjamin M., 2016. The Scenario Model Intercomparison Project (ScenarioMIP) for CMIP6. *Geosci. Model Dev.* 9 (9), 3461–3482.
- OEH, 2014. Soil condition and land management in New South Wales: final results from the 2008–09 monitoring, evaluation and reporting program. OEH Technical Report, NSW Office of Environment and Heritage, Sydney.
- Olaya-Abril, Alfonso, Parras-Alcántara, Luis, Lozano-García, Beatriz, Obregón-Romero, Rafael, 2017. Soil organic carbon distribution in Mediterranean areas under a climate change scenario via multiple linear regression analysis. *Sci. Total Environ.* 592, 134–143.
- Padarian, José, Minasny, Budiman, McBratney, Alex B., 2020. Machine learning and soil sciences: a review aided by machine learning tools. *SOLI* 6 (1), 35–52.
- Quiñonero-Candela, J., Sugiyama, M., Lawrence, N.D., Schwaighofer, A., 2009. Dataset shift in machine learning. Mit Press.
- Rayment, G.E., Lyons, D., 2011. *Soil Chemical Methods - Australasia*. CSIRO Publishing, Collingwood, Victoria Australia.
- R Core Team R: A language and environment for statistical computing. R Foundation for Statistical Computing 2020 Vienna, Austria. (<https://www.r-project.org/>).
- Reyes Rojas, Luis A., Adhikari, Kabindra, Ventura, Stephen J., 2018. Projecting Soil Organic Carbon Distribution in Central Chile under Future Climate Scenarios. *J. Environ. Qual.* 47 (4), 735–745.
- Rial, M., Martínez Cortizas, A., Taboada, T., Rodríguez-Lado, L., 2017. Soil organic carbon stocks in Santa Cruz Island, Galapagos, under different climate change scenarios. *CATENA* 156, 74–81.
- Robertson, Fiona, Crawford, Doug, Partington, Debra, Oliver, Ivanah, Rees, David, Aumann, Colin, Armstrong, Roger, Perris, Roger, Davey, Michelle, Moodie, Michael, Baldock, Jeff, 2016. Soil organic carbon in cropping and pasture systems of Victoria, Australia. *Soil Res.* 54 (1), 64. <https://doi.org/10.1071/SR15008>.
- Sanderman, J., Baldock, J., Hawke, B., Macdonald, L., Puccini, A., Szarvas, S. (2011) National soil carbon research programme: field and laboratory methodologies.
- Michael W. I. Schmidt Margaret S. Torn Samuel Abiven Thorsten Dittmar Georg Guggenberger Ivan A. Janssens Markus Kleber Ingrid Kögel-Knabner Johannes Lehmann David A. C. Manning Paolo Nannipieri Daniel P. Rasse Steve Weiner Susan E. Trumbore Persistence of soil organic matter as an ecosystem property *Nature* 478 7367 2011 49 56.
- Pete Smith Soils and climate change *Current Opinion in Environmental Sustainability* 4 5 2012 539 544.
- Soleimani, Azam, Hosseini, Seyed Mohsen, Massah Bavani, Ali Reza, Jafari, Mostafa, Francaviglia, Rosa, 2017. Simulating soil organic carbon stock as affected by land cover change and climate change, Hyrcanian forests (northern Iran). *Sci. Total Environ.* 599–600, 1646–1657.
- Somarathna, P.D.S.N., Malone, B.P., Minasny, B., 2016. Mapping soil organic carbon content over New South Wales, Australia using local regression kriging. *Geoderma Regional* 7 (1), 38–48.
- Uta Stockmann Mark A. Adams John W. Crawford Damien J. Field Nilusha Henakaarchchi Meaghan Jenkins Budiman Minasny Alex B. McBratney Vivien de Remy de Courcelles Kanika Singh Ichsan Wheeler Lynette Abbott Denis A. Angers Jeffrey Baldock Michael Bird Philip C. Brookes Claire Chenu Julie D. Jastrow Rattan Lal Johannes Lehmann Anthony G. O'Donnell William J. Parton David Whitehead Michael Zimmermann The knowns, known unknowns and unknowns of sequestration of soil organic carbon *Agriculture, Ecosystems & Environment* 164 2013 80 99.
- Sulman, Benjamin N., Phillips, Richard P., Oishi, A., Christopher, Sheviakova, Elena, Pacala, Stephen W., 2014. Microbe-driven turnover offsets mineral-mediated storage of soil carbon under elevated CO<sub>2</sub>. *Nat. Clim. Change* 4 (12), 1099–1102.
- A.M. Ukkola M.G. De Kauwe M.L. Roderick G. Abramowitz A.J. Pitman Robust Future Changes in Meteorological Drought in CMIP6 Projections Despite Uncertainty in Precipitation *Geophysical Research Letters* 47:e2020GL087820 2020.
- R. A. Viscarra Rossel Fine-resolution multiscale mapping of clay minerals in Australian soils measured with near infrared spectra *Journal of Geophysical Research: Earth Surface* 116 F4 2011 10.1029/2011JF001977.
- Viscarra Rossel, Raphael A., Webster, Richard, Bui, Elisabeth N., Baldock, Jeff A., 2014. Baseline map of organic carbon in Australian soil to support national carbon accounting and monitoring under climate change. *Glob. Change Biol.* 20 (9), 2953–2970.
- Wadoux, Alexandre M.J.-C., Minasny, Budiman, McBratney, Alex B., 2020. Machine learning for digital soil mapping: Applications, challenges and suggested solutions. *Earth Sci. Rev.* 210, 103359. <https://doi.org/10.1016/j.earscirev.2020.103359>.
- Wang, Bin, Waters, Cathy, Orgill, Susan, Gray, Jonathan, Cowie, Annette, Clark, Anthony, Liu, De Li, 2018a. High resolution mapping of soil organic carbon stocks using remote sensing variables in the semi-arid rangelands of eastern Australia. *Sci. Total Environ.* 630, 367–378.
- Wang, Bin, Zheng, Lihong, Liu, De Li, Ji, Fei, Clark, Anthony, Yu, Qiang, 2018b. Using multi-model ensembles of CMIP5 global climate models to reproduce observed monthly rainfall and temperature with machine learning methods in Australia. *Int. J. Climatol.* 38 (13), 4891–4902.
- Shuai Wang Qianlai Zhuang Qiubing Wang Xinxin Jin Chunlan Han Mapping stocks of soil organic carbon and soil total nitrogen in Liaoning Province of China *Geoderma* 305 2017 250 263.
- Waters, C.M., Melville, G.J., Orgill, S.E., Alemseged, Y., 2015. The relationship between soil organic carbon and soil surface characteristics in the semi-arid rangelands of southern Australia. *The Rangeland J.* 37, 297–307.
- Waters, C.M., Orgill, S.E., Melville, G.J., Too, I.D., Smith, W.J., 2016. Management of Grazing Intensity in the Semi-Arid Rangelands of Southern Australia: Effects on Soil and Biodiversity. *Land Degrad. Dev.* 28, 1363–1375.
- Wilford, John, 2012. A weathering intensity index for the Australian continent using airborne gamma-ray spectrometry and digital terrain analysis. *Geoderma* 183–184, 124–142.
- WMO, 2017. *WMO guidelines on the calculation of climate normals*. World Meteorological Organization Geneva, Switzerland.
- Wu, Gao-Lin, Liu, Yu, Tian, Fu-Ping, Shi, Zhi-Hua, 2017. Legumes Functional Group Promotes Soil Organic Carbon and Nitrogen Storage by Increasing Plant Diversity. *Land Degrad. Dev.* 28 (4), 1336–1344.
- Yang, Ren-Min, Zhang, Gan-Lin, Liu, Feng, Lu, Yuan-Yuan, Yang, Fan, Yang, Fei, Yang, Min, Zhao, Yu-Guo, Li, De-Cheng, 2016. Comparison of boosted regression tree and random forest models for mapping topsoil organic carbon concentration in an alpine ecosystem. *Ecol. Ind.* 60, 870–878.
- Yigini, Yusuf, Panagos, Panos, 2016. Assessment of soil organic carbon stocks under future climate and land cover changes in Europe. *Sci. Total Environ.* 557–558, 838–850.
- Zhou, Yin, Hartemink, Alfred E., Shi, Zhou, Liang, Zongzheng, Lu, Yanli, 2019. Land use and climate change effects on soil organic carbon in North and Northeast China. *Sci. Total Environ.* 647, 1230–1238.